Journal of Organometallic Chemistry, 438 (1992) 353–369
Elsevier Sequoia S.A., Lausanne
JOM 22833

Indenyl carbametallaboranes

III *. The synthesis and characterization of novel rhodium carbaborane compounds with 3-(C_2B_9)-8-{(C_9H_6)Rh(C_9H_7)}-3,1,2-*closo*-RhC_2B_9, 10-{(C_9H_6)Rh(C_9H_7)}-7,8-*nido*-C_2B_9, 9-{(C_9H_6)Rh(C_9H_7)}-7,8-*nido*-C_2B_9 and 3-(η-C_9H_7)-3,1,2-*closo*-RhC_2B_9 structures

Zoe G. Lewis and Alan J. Welch
Department of Chemistry, University of Edinburgh, Edinburgh EH9 3JJ (UK)

(Received April 7, 1992)

Abstract

When $RhCl_3 \cdot 3H_2O$ and indene are refluxed in methanol a brown solid, $[(C_9H_7)RhCl_2]_x$, is deposited. This, in turn, reacts with a suspension of Tl_2[7,8-*nido*-$C_2B_9H_{11}$] in CH_2Cl_2 to afford three products, 3-($C_2B_9H_{11}$)-8-{(C_9H_6)Rh(C_9H_7)}-3,1,2-*closo*-Rh$C_2B_9H_{10}$ (**Ia**), 10-{(C_9H_6)Rh(C_9H_7)}-7,8-*nido*-$C_2B_9H_{11}$ (**IIa**) and 9-{(C_9H_6)Rh(C_9H_7)}-7,8-*nido*-$C_2B_9H_{11}$ (**IIIa**). In **Ia**, which was characterized spectroscopically and crystallographically, a {*closo*-($C_2B_9H_{11}$)Rh($C_2B_9H_{10}$)} fragment is bonded to a {(C_9H_6)Rh(C_9H_7)} fragment *via* a B(8)–C bond, whereas in **IIa** and **IIIa**, which were characterized spectroscopically, the same organometallic fragment is linked to, respectively, B(10) and B(9) of a {7,8-*nido*-$C_2B_9H_{11}$} unit. Reaction of $[(C_9H_7)RhCl_2]_x$ with Tl_2[7-(CH_2OCH_3)-7,8-*nido*-$C_2B_9H_{10}$] gives rise to a single isolatable product of 7-CH_2OCH_3-10-{(C_9H_6)Rh(C_9H_7)}-7,8-*nido*-$C_2B_9H_{10}$ (**IIb**) shown to be a simple analogue of **IIa** by NMR spectroscopic study. An analogue of **IIIa**, namely 7-Ph-9/11-{(C_9H_6)Rh(C_9H_7)}-7,8-*nido*-$C_2B_9H_{10}$ (**IIId**) is one of the two products isolated following the reaction between $[(C_9H_7)RhCl_2]_x$ and Tl_2[7-Ph-7,8-*nido*-$C_2B_9H_{10}$], the other being the *closo* carbametallaborane, 1-Ph-3-(C_9H_7)-3,1,2-*closo*-Rh$C_2B_9H_{10}$ (**IVd**) characterized by unit cell and space group determination. A structural analogue, 1,2-$(CH_2OCH_3)_2$-3-(C_9H_7)-3,1,2-*closo*-Rh$C_2B_9H_9$ (**IVc**) is the only product isolated from the reaction of $[(C_9H_7)RhCl_2]_x$ with Tl_2[7,8-$(CH_2OCH_3)_2$-7,8-*nido*-$C_2B_9H_9$]. The structural characterization of each of these novel rhodium carbaborane species is discussed, and the implications of their structures on the nature of $[(C_9H_7)RhCl_2]_x$ is considered.

Correspondence to: Dr. A.J. Welch.

* For Parts I and II, see refs. 1 and 2.

Introduction

Previous papers in this series [1,2] have described the synthesis and structural characterization of a family of indenyl carbacobaltaboranes, 1-R′-2-R″-3-(η-C_9H_7)-3,1,2-*closo*-$CoC_2B_9H_9$, R′ = R″ = H [1]; R′ = CH_2OCH_3, R″ = H [2]; R′ = R″ = CH_2OCH_3 [2]; R′ = Ph, R″ = H [2]. By these studies, we have been able to demonstrate that (i) in the parent compound (R′ = R″ = H), the theoretically predicted *cisoid* conformation, the preference for which may be readily understood in terms of simple *trans* influence arguments, is experimentally observed; (ii) 1-ether or 1-phenyl substitution does not significantly perturb this conformation, and (iii) in contrast, 1,2-diether substitution results in a conformational change such that the next-best staggered conformation (as defined by the two metalla-bonded pentagonal rings) is adopted to avoid unfavourable steric crowding between the indenyl 6-membered ring and the carbaborane cage substituents.

The above carbacobaltaboranes are afforded by reaction between $Co(acac)_3$ (acac = acetylacetonate), Tl_2[carbaborane] and Li[C_9H_7] in tetrahydrofuran (THF), a route analogous to that which had previously been used [3,1] to synthesize 3-Cp-*closo*-3,1,2-$CoC_2B_9H_{11}$ [Cp = (η-C_5H_5)]. Yields by this method are poor to modest, typically 15% at best, and accordingly we have sought an alternative route to d^6 indenyl carbametallaboranes. Since $[CpRhCl_2]_n$ [4,5] and $[Cp^*RhCl_2]_2$ [5] [Cp* = (η-C_5Me_5)] are well-known reagents for introducing the {CpRh} and {Cp*Rh} fragments, respectively, into a wide variety of organometallic compounds, including metallaboranes and carbametallaboranes [6–8] in good yields, we reasoned that the analogous indenyl species could be an interesting and potentially useful reagent.

In this paper, we report the synthesis of the reagent $[(C_9H_7)RhCl_2]_x$, and the results of its reactions with a variety of carbaborane anions. The latter have afforded a number of novel rhodium carbaborane species, structural elucidation of which by NMR spectroscopy and/or X-ray crystallography allows speculation on the nature of $[(C_9H_7)RhCl_2]_x$.

Experimental

Synthesis and characterization

Reactions were carried out under dry nitrogen by standard Schlenk line techniques, with some subsequent manipulations in the open laboratory. Solvents were dried and distilled under nitrogen prior to use. IR spectra were recorded as CH_2Cl_2 solutions or as KBr pellets on a Perkin–Elmer 598 spectrophotometer. NMR spectra were recorded on Bruker WH360 or Varian Associates VXR600 spectrometers as $CDCl_3$, CD_2Cl_2 or $(CD_3)_2CO$ solutions at 298 K. Chemical shifts are reported relative to external $SiMe_4$ (^1H) or $BF_3 \cdot OEt_2$ (^{11}B). Microanalyses were performed by the departmental service. The starting materials Tl_2[7,8-*nido*-$C_2B_9H_{11}$] [9], Tl_2[7-(CH_2OCH_3)-7,8-*nido*-$C_2B_9H_{10}$] [10], Tl_2[7,8-$(CH_2OCH_3)_2$-7,8-*nido*-$C_2B_9H_9$] [10] and Tl_2[7-Ph-7,8-*nido*-$C_2B_9H_{10}$] [11] were prepared as previously described. $RhCl_3 \cdot 3H_2O$ (Johnson Matthey) was used as supplied and indene (BDH) was distilled before use.

Synthesis of $[(C_9H_7)RhCl_2]_x$

Typically, a mixture of $RhCl_3 \cdot 3H_2O$ (2 g, 7.6 mmol) and freshly distilled indene (3.5 cm^3, 30.1 mmol) was refluxed in methanol (50 cm^3) for 15 h, during which a brown solid was deposited. This was filtered off, washed successively with methanol (2 × 10 cm^3) and ether (2 × 10 cm^3), and dried *in vacuo*. Further refluxing (15 h) of the original filtrate afforded a second crop of solid material which was similarly recovered. Combined yield 43%. Anal. Found: C, 36.7; H, 2.74. $C_{18}H_{14}Cl_4Rh_2$ calc.: C, 37.4; H, 2.42%. IR ν_{max} at 3100br, 3050br, sh, 2960m, 2930w (all C–H), 1515w, 1450m, 1440m, 1385m, 1335s, 1260w, 885m, 835m br, 750sh, 745s, 735sh, 570m, 490m, 340sh, 335sh, 325m.

Reaction between $[(C_9H_7)RhCl_2]_x$ *and* $Tl_2[7,8\text{-nido-}C_2B_9H_{11}]$

To a solid mixture of $[(C_9H_7)RhCl_2]_x$ (0.101 g, 0.175 mmol) and $Tl_2[7,8\text{-}nido\text{-}C_2B_9H_{11}]$ (0.203 g, 0.35 mmol) at −196°C, was added CH_2Cl_2 (10 cm^3). The mixture was allowed to warm to room temperature with stirring. After 2.5 h, the mixture was filtered under nitrogen and the brown filtrate evaporated *in vacuo* to give a dark brown solid. Preparative TLC (CH_2Cl_2 : hexane eluant, 3 : 1) afforded three main bands, yellow (R_f *ca.* 0.8), apricot (R_f *ca.* 0.6) and orange (R_f *ca.* 0.5), each of which was collected and recrystallized (CH_2Cl_2 : hexane, 1 : 3, −30°C) to afford microcrystals of the rhodium carbaborane compounds **Ia**, **IIa**, and **IIIa**, respectively.

*$3\text{-}(C_2B_9H_{11})\text{-}8\text{-}\{(C_9H_6)Rh(C_9H_7)\}\text{-}3,1,2\text{-closo-}RhC_2B_9H_{10}$ (**Ia**).* Yield 4%. Anal. Found: C, 38.2; H, 5.09. $C_{22}H_{34}B_{18}Rh_2$ calc.: C, 37.81; H, 4.9%. IR ν_{max} at 2555 cm^{-1} (B–H). ^1H NMR (CD_2Cl_2): δ 7.20 (m, 4H, *H*(25–28)); 6.50 (m, 4H, *H*(15–18)); 5.92 (d, 2H, *H*(21,23)); 5.84 (s, 2H, *H*(11,13)); 5.79 (t of d, ^3J(HH) = 3 Hz, $^?J$(HH) = 1 Hz, 1H, *H*(22)); 3.80 (s, 2H, cage-C*H*); 3.71 (s, 2H, cage-C*H*) ppm $^{11}B\text{-}\{^1H\}$: See Table 1 for chemical shifts and assignments via $^{11}B\text{–}^{11}B$ COSY spectrum.

*$10\text{-}\{(C_9H_6)Rh(C_9H_7)\}\text{-}7,8\text{-nido-}C_2B_9H_{11} \cdot 0.5CH_2Cl_2$ (**IIa**).* Yield 8%. Anal. Found: C, 49.3; H, 4.93. $C_{20.5}H_{25}B_9ClRh$ calc.: C, 48.6, H, 4.97%. IR ν_{max} at 2520 cm^{-1} (B–H). ^1H NMR (CD_2Cl_2): δ 7.23 (m, 2H) and 7.18 (m, 2H) [*H*(25–28)]; 6.65 (m, 2H) and 6.58 (m, 2H) [*H*(15–18)]; 6.01 (d, ^3J(HH) = 3 Hz, 2H, *H*(21,23)); 5.92 (t, ^3J(HH) = 3 Hz, 1H, *H*(22)); 5.91 (s, 2H, *H*(11,13)); 2.10 (s, 2H, *H*(7C,8C)); −1.54 (q, 1H, $H(10B_{endo})$) ppm. $^{11}B\text{-}\{^1H\}$: δ −9.60 (2B, *B*(9,11)); −13.77 (2B, *B*(5,6)); −17.81 (1B, *B*(3)); −20.79 (2B, *B*(2,4)); −26.39 (1B, *B*(10)); −37.08 (1B, *B*(1)) ppm $^1H\text{-}\{^{11}B_{selective}\}$: δ 2.21 (s, 2H, *H*(9B,11B)); 1.56 (s, 2H, *H*(5B,6B)); 1.85 (s, 1H, *H*(3B)); 1.40 (s, 2H, *H*(2B,4B)); 0.68 (s, 1H, *H*(1B)) ppm.

$9\text{-}\{(C_9H_6)Rh(C_9H_7)\}\text{-}7,8\text{-nido-}C_2B_9H_{11} \cdot 0.5CH_2Cl_2$ (**IIIa**). Yield 6%. Anal. Found: C, 48.6; H, 5.05. $C_{20.5}H_{25}B_9ClRh$ calc.: C, 48.6; H, 4.97%. IR ν_{max} at 2520 cm^{-1} (B–H). ^1H NMR (CD_2Cl_2): δ 7.22 (m, 4H, *H*(25–28)); 6.65 (m, 4H, *H*(15–18)); 6.07 (s, 1H, *H*(11 or 13)); 6.01 (d, ^3J(HH) = 3 Hz, 2H, *H*(21 or 23)); 6.00 (d, ^3J(HH) = 4 Hz, 1H, *H*(23 or 21)); 5.97 (s, 1H, *H*(11 or 13)); 5.82 (d of d, ^3J(HH) = 4 Hz, 3 Hz, 1H, *H*(22)); 2.45 (s, 1H, *H*(7C or 8C)); 2.10 (s, 1H, *H*(8C or 7C)); −2.60 (v br, 1H, $H(10B_{endo})$) ppm. $^{11}B\text{-}\{^1H\}$: δ −4.14 (1B, *B*(9)); −5.10 (1B); −13.74 (1B); −16.16 (1B); −17.16 (1B); −20.82 (1B); −24.86 (1B); −29.45 (1B, *B*(10)); −35.15 (1B) ppm. $^1H\text{-}\{^{11}B_{selective}\}$: δ 2.16 (s, 1H); 1.90 (s, 1H); 1.75 (s, 1H); 1.86 (s, 1H); 1.16 (s, 1H); 0.90 (s, 1H); 0.59 (s, 1H, $H(10B_{exo})$); 0.80 (s, 1H) ppm.

Reaction between $[C_9H_7RhCl_2]_x$ *and* $Tl_2[7\text{-}(CH_2OCH_3)\text{-}7,8\text{-nido-}C_2B_9H_{10}]$

Similarly, $[(C_9H_7)RhCl_2]_x$ (0.100 g, 0.173 mmol) and $Tl_2[7\text{-}(CH_2OCH_3)\text{-}7,8\text{-}\textit{nido}\text{-}C_2B_9H_{10}]$ (0.202 g, 0.346 mmol) were allowed to react in CH_2Cl_2 (15 cm^3). The mixture was warmed to room temperature, stirred for 40 min then filtered to give a dark green solution. Preparative TLC (CH_2Cl_2 : THF : hexane eluant, 3 : 1 : 1) gave an orange band (R_f *ca.* 0.85), which yielded microcrystals of compound $7\text{-}CH_2OCH_3\text{-}10\text{-}\{(C_9H_6)Rh(C_9H_7)\}\text{-}7,8\text{-}\textit{nido}\text{-}C_2B_9H_{10} \cdot CH_2Cl_2$ (**IIb**). Yield 5%. Anal. Found: C, 46.9; H, 4.96. $C_{23}H_{31}B_9Cl_2ORh$ calc.: C, 46.8; H, 5.18%. IR ν_{max} at 2540 cm^{-1} (B–H). ^1H NMR (CD_2Cl_2): δ 7.23 (m, 2H) and 7.18 (m, 2H) [*H*(25–28)]; 6.66 (m, 2H) and 6.58 (m, 2H) [*H*(15–18)]; 6.01 (d, $^3J(HH) = 3\ H_3$, 1H) and 6.00 (d, $^3J(HH) = 3$ Hz, 1H) [*H*(21,23)]; 5.92 (s, 3H, coincidence); 3.60 and 3.26 (AB, $^2J(HH) = 10$ Hz, 2H, $-CH_2-O$); 3.32 (s, 3H, $-O-CH_3$); 2.14 (s, 1H, *H*(8C)); −1.40 (br q, 1H, $H(10B_{endo})$) ppm. $^{11}B\text{-}\{^1H\}$: δ −9.20 (1B); −10.02 (1B); −13.89 (1B); −14.85 (1B); −15.50 (1B); −17.64 (1B); −21.40 (1B); −26.36 (1B); −36.91 (1B) ppm. $[(CD_3)_2CO]$ ^1H (region between δ 6.4 and 5.8 ppm only): δ 6.25 (d, $^3J(HH) = 2$ Hz, 1H) and 6.24 (d, $^3J(HH) = 3$ Hz, 1H) [*H*(21,23)]; 5.95 (s, 2H, *H*(11,13) coincidence); 5.93 (d of d, $^3J(HH) = 3$ Hz, 2 Hz, 1H, *H*(22))] ppm.

Reaction between $[(C_9H_7)RhCl_2]_x$ *and* $Tl_2[7\text{-}Ph\text{-}7,8\text{-nido-}C_2B_9H_{10}]$

Similarly, $[(C_9H_7)RhCl_2]_x$ (0.104 g, 0.18 mmol) and $Tl_2[7\text{-}Ph\text{-}7,8\text{-}\textit{nido}\text{-}C_2B_9H_{10}]$ (0.21 g, 0.36 mmol) were allowed to react in CH_2Cl_2 (15 cm^3). The mixture was allowed to warm to room temperature, stirred for 15 h and filtered, to give an olive-green solution. Preparative TLC (CH_2Cl_2: hexane eluant, 4 : 1) gave olive minor (R_f *ca.* 0.95) and orange major (R_f *ca.* 0.85) bands. The product isolated from the first band was crystallized by slow evaporation of a CH_2Cl_2 solution to give small crystals, subsequently shown by unit cell and space group determination to be $1\text{-}Ph\text{-}3\text{-}(C_9H_7)\text{-}3,1,2\text{-}\textit{closo}\text{-}RhC_2B_9H_{10}$ (**IVd**), by analogy with the previously characterized cobalt analogue [2]. The product from the second band was recovered as solid $7\text{-}Ph\text{-}9/11\text{-}\{(C_9H_6)Rh(C_9H_7)\}\text{-}7,8\text{-}\textit{nido}\text{-}C_2B_9H_{10}$ (**IIId**). Yield 2%. IR ν_{max} at 2535 cm^{-1} (B–H). ^1H NMR (CD_2Cl_2): δ 7.33 (m, 2H, *H*(72,76)); 7.18 (m, 6H, *H*(73,75,25–28) coincidence); 7.07 (m, 1H, *H*(74)); 6.65 (m, 4H, *H*(15–18)); 6.15 (s, 1H, *H*(11 or 13)); 5.99 (d, $^3J(HH) = 3$ Hz, 1H, *H*(21 or 23)); 5.96 (s, 1H, *H*(13 or 11)); 5.95 (d, $^3J(HH) = 3$ Hz, 1H, *H*(23 or 21)); 5.84 (d of d (app t), $^3J(HH) = 3$ Hz, 3 Hz, 1H, *H*(22)); 2.79 (s, 1H, *H*(8C)); −2.30 (v br, 1H, $H(10B_{endo})$) ppm. $^{11}B\text{-}\{^1H\}$: δ −4.29 (2B, coincident); −11.79 (1B); −12.50 (1B); −13.42 (1B); −20.74 (1B); −25.36 (1B); −28.39[1B, *B*(10)]; −32.76 (1B) ppm.

Reaction between $[(C_9H_7)RhCl_2]_x$ *and* $Tl_2[7,8\text{-}(CH_2OCH_3)_2\text{-}7,8\text{-nido-}C_2B_9H_9]$

Similarly a mixture of $[(C_9H_7)RhCl_2]_x$ (0.18 g, 0.31 mmol) and $Tl_2[7,8\text{-}(CH_2OCH_3)_2\text{-}7,8\text{-}\textit{nido}\text{-}C_2B_9H_9]$ (0.39 g, 0.62 mmol) in CH_2Cl_2 (20 cm^3) was allowed to warm with stirring. After 15 h the solution was filtered, and the filtrate evaporated *in vacuo* to yield a purple solid. Preparative TLC (CH_2Cl_2 eluant) afforded $1,2\text{-}(CH_2OCH_3)_2\text{-}3\text{-}(C_9H_7)\text{-}3,1,2\text{-}\textit{closo}\text{-}RhC_2B_9H_9$ (**IVc**) as a yellow solid. Yield 1%. IR ν_{max} at 2530 cm^{-1} (B–H). ^1H NMR ($CDCl_3$): δ 7.36 (b app s, 4H, *H*(35–38)); 6.46 (d, $^3J(HH) = 3$ Hz, 2H, *H*(31,33)); 5.88 (t of d, $^3J(HH) = 3$ Hz, $^{?}J(HH) = 1.5$ Hz, 1H, *H*(32)); 3.22 (s, 6H, $-O-CH_3$); 2.89 and 2.86 (AB, $^2J(HH) =$ 12 Hz, 4H, $-CH_2-O$) ppm. $^{11}B\text{-}\{^1H\}$: δ 10.72 (1B); 5.06 (1B); −0.10 (2B); −6.56 (2B); −14.21 (2B); −19.85 (1B) ppm.

Crystallographic studies

All measurements were carried out on an Enraf–Nonius CAD4 diffractometer equipped with graphite-monochromated Mo-K_α X-radiation ($\lambda_{bar} = 0.71069$ Å) and a ULT-1 low temperature device (nitrogen stream).

3-($C_2B_9H_{11}$)-8-{(C_9H_6)Rh(C_9H_7)}-3,1,2-closo-*$RhC_2B_9H_{10}$.(**Ia**).* A single crystal ($0.1 \times 0.1 \times 0.02$ mm^3) was mounted in a Lindemann tube on the diffractometer, and unit cell and orientation matrix determined from the least-squares refinement of the setting angles of 25 centred reflections ($2 < \theta < 11°$).

Crystal data were as follows. $C_{22}H_{34}B_{18}Rh_2$, $M = 698.91$, orthorhombic, space group *Pbca*, $a = 12.296(8)$, $b = 19.69(4)$, $c = 29.030(18)$ Å, $V = 7028.8$ Å^3, $T = 185 \pm 1$ K, $Z = 8$, $D_{calc.} = 1.321$ g cm^{-3}, μ(Mo-K_α) = 9.38 cm^{-1}, $F(000) = 2768$ (D_{calc}, μ and $F(000)$ assumed no solvate).

Almost three symmetry-independent octants of data were collected for $1 \le \theta \le 15°$ (the limit of measurable diffraction for this small crystal) in the ranges $h -8 \to +8$, $k -14 \to +14$, l $0 \to +15$) by ω–2θ scans (ω scan width $0.8 + 0.34 \tan \theta$). No crystal movement or decay was detected during the 111 h of data collection. Of 4140 reflections measured, 1759 [$F \ge 2.0\sigma(F)$] were retained.

The structure was solved by direct methods (SHELX86 [12]) and developed by iterative full-matrix least-squares refinement (SHELX76 [13]). C(1) and C(2) were identified as cage carbon by a combination of refined (as B) isotropic thermal parameters and internuclear distances, and the results agree with the conclusion from the NMR studies that this cage is substituted at B(8). C(1′) was identified by its refined (as B) isotropic thermal parameter, but definitive location of the other cage carbon atom in the primed cage was not possible, and sites (2′) and (4′) were assigned occupancies of 5.5 e [(B + C)/2]. Indenyl H atoms were set in calculated positions, riding on their respective C atoms, and given an invariant U value of 0.07 Å^2. Cage H atoms were not located. Separate group isotropic thermal parameters were employed for all indenyl C atoms, and all non-Rh cage atoms. Following isotropic convergence, an empirical absorption correction was applied and data were then merged to afford 985 unique reflections, $R_{merge} = 0.038$. Rhodium atoms were allowed anisotropic thermal motion, and in the final stages, data were weighted according to $w^{-1} = [\sigma^2(F) + 0.00168F^2]$. **Ia** crystallizes with badly disordered solvate molecules, the best model of which involved 8 carbon atoms with fixed U of 0.04 Å^2 and a (common) refined population parameter of 0.614(24). Even this model, however, does not represent a chemically recognizable fragment of either CH_2Cl_2 or hexane. $R = 0.1072$, $R_w = 0.1210$, $S = 1.319$ for 167 variables. $U_{indenyl\text{-}C} = 0.044(5)$ Å^2, $U_{cage\text{-}B/C} = 0.041(5)$ Å^2. Maximum and minimum residues in final ΔF synthesis were 1.10 and -0.8 e Å^{-3}, respectively.

Atomic scattering factors for B, C and H were those incorporated in SHELX76, and those for Rh were taken from *International Tables* [14]. Programs used in addition to those cited above were CADABS [15], DIFABS [16], CALC [17] and EASYORTEP [18]. Table 2 lists coordinates of refined atoms. Calculated H atom coordinates, thermal parameters, a full list of bond distances and interbond angles, and tables of F_o/F_c values are available form A.J.W.

1-Ph-3-(C_9H_7)-3,1,2-closo-*$RhC_2B_9H_{10}$ (**IVd**).* A small ($0.1 \times 0.1 \times 0.05$ mm^3) diamond-shaped crystal of **IVd** was mounted in a Lindemann tube and set on the diffractometer. Setting was achieved via 25 centred reflections with θ values between 3° and 8°.

Crystal data were as follows. $C_{17}H_{22}B_9Rh$, $M = 426.56$, monoclinic, space group $C2/c$, $a = 17.710(16)$, $b = 13.214(8)$, $c = 18.81(3)$ Å, $\beta = 119.86(10)^\circ$, $V = 7028.8$ Å^3, $T = 291 \pm 1$ K, $Z = 8$, $D_{\text{calc.}} = 1.484$ g cm^{-3}, $\mu(\text{Mo-}K_\alpha) = 8.78$ cm^{-1}, $F(000) = 1712$.

The compound is isomorphous with its previously characterized cobalt analogue [2] and this fact, coupled with the weakness of its diffraction, means that data collection is not justified.

Results and discussion

The reaction between rhodium trichloride and indene in refluxing methanol yields a light brown solid whose microanalytical data are consistent with the formulation $[(C_9H_7)RhCl_2]_x$. The reaction is fully analogous with that which affords the polymeric species $[(C_5H_5)RhCl_2]_n$ from $RhCl_3$ and C_5H_6 [5], but whereas this latter product is effectively insoluble in all common organic solvents, $[(C_9H_7)RhCl_2]_x$ is partially soluble in, for example, CH_2Cl_2. This allows the very obvious assertion that the degree of association of the indenyl species $[(C_9H_7)RhCl_2]_x$ may lie between that of the truly polymeric Cp analogue and the dimeric Cp* analogue. However, analysis of some of the products of the reactions of $[(C_9H_7)RhCl_2]_x$ with *nido* carbaborane anions suggests a rather more complex description, as discussed below.

When $[(C_9H_7)RhCl_2]_x$ is allowed to react with $Tl_2[C_2B_9H_{11}]$ in CH_2Cl_2, three products may be isolated following work-up. The most mobile of these, **Ia**, was isolated as a yellow microcrystalline material, microanalytical data for which were consistent with one indenyl ligand to one rhodium atom to one carbaborane cage. However, spectroscopic investigation quickly revealed that the product was not the expected indenyl carbarhodaborane 3-(η-C_9H_7)-3,1,2-*closo*-$RhC_2B_9H_{11}$.

Thus, in the ^1H NMR spectrum (recorded in CD_2Cl_2), there is clear evidence for more than one type of indenyl ligand. A multiplet of integral 4H centred on 7.2 ppm, a doublet (3 Hz) of integral 2H at 5.92 ppm and a lower frequency triplet (3 Hz) of weak doublets (1 Hz) of integral 1H, are collectively indicative of an η^5-bonded (C_9H_7) ligand; in addition, a lower frequency multiplet (4H) centred on 6.5 ppm and a singlet (2H) at 5.84 ppm were observed indicative of a (C_9H_6) ligand derived from (C_9H_7) by substitution of the symmetry-unique H atom. Note that the multiplets of integral 4H were assigned to (C_9H_7) and (C_9H_6) ligands by NOE experiments.

At lower frequency in the ^1H NMR spectrum of **Ia** there are two broad resonances, each corresponding of two H atoms, assigned to cage CH atoms. This suggests either that two different $\{C_2B_9\}$ fragments exist within the molecule each having C_s symmetry at least on the NMR time scale, or that there are two identical cages each of which is rendered asymmetric. Only the former is supported by the observation of 12 resonances, in the ratio 1:1:1:1:2:2:2:2:2:2:1:1, in the ^{11}B-$\{^1H\}$ NMR spectrum. Moreover, in the proton-coupled ^{11}B spectrum, only 11 of the 12 resonances exhibit the doublet coupling ($^1J(BH) = 120$–155 Hz) typical of an exopolyhedral {BH} unit, the exception being the highest frequency signal (9.19 ppm). Taken together with the ^1H NMR data, this suggests the presence of one $(C_2B_9H_{11})$ and one $(C_2B_9H_{10}[C_9H_6])$ cage ligand in **Ia**, the latter involving an exopolyhedral B–C 2c–2e bond.

Table 1

^{11}B chemical shifts (ppm) in 3-Cp*-3,1,2-*closo*-$RhC_2B_9H_{11}$ [a] and in **Ia**

Atom	3-Cp*-3,1,2-*closo*-$RhC_2B_9H_{11}$	**Ia** (substituted cage)	**Ia** (unsubstituted cage)
8	+8.6	+9.2	+9.0
10	−1.8	+2.3	+3.9
4,7	−3.5	−5.5	−3.5
9,12	−8.3	−4.5	−6.1
5,11	−18.6	−17.9	−16.1
6	−23.4	−21.2	−22.8

[a] From ref. 8.

Individual ^{11}B resonances in **Ia** were assigned by analysis of an $^{11}B-^{11}B$ COSY spectrum and are listed in Table 1 for both the unsubstituted and substituted cages. Also given are (assigned [8]) ^{11}B chemical shifts in 3-Cp*-3,1,2-*closo*-$RhC_2B_9H_{11}$. The generally good correlation of these with those in **Ia** strongly suggests that each of the two different $\{C_2B_9\}$ cages in the latter is bound in normal, η^5, fashion to a Rh^{III} centre. Moreover, it is clear that cage substitution in **Ia** has occurred at the B(8) atom.

The combined spectroscopic data for **Ia** show it to be $(C_9H_7)Rh_2(C_2B_9H_{11})(C_2B_9H_{10}[C_9H_6])$, but do not distinguish between the two possible structures depicted in Fig. 1. Numerous attempts to grow crystals suitable for an X-ray diffraction study were unsuccessful until eventually an extremely small, but well-formed, single crystal was obtained by diffusion of hexane into a THF solution of the compound. The effective limit for diffraction was found to be *ca.* 15° (Mo-K_α X-radiation) and so to improve the accuracy of the experiment, almost three octants of symmetry-independent data were collected. Although the structure was easily solved, refinement was hampered by the general paucity of data and by the presence of greatly disordered solvent molecules (see Experimental section), so that the accuracy of the final model (Table 2 for atomic coordinates, Table 3 for internuclear distances and selected interbond angles) is far from ideal. Nevertheless, the molecular structure of **Ia** is unambiguously established.

Figure 2 shows a perspective view of a single molecule and demonstrates the atomic numbering scheme adopted. Thus **Ia** is the novel zwitterionic compound 3-$(C_2B_9H_{11})$-8-$\{(C_9H_6)Rh(C_9H_7)\}$-3,1,2-*closo*-$RhC_2B_9H_{10}$, formally derived from $[Rh(C_2B_9H_{11})_2]^-$ and $[Rh(C_9H_7)_2]^+$ by loss of 2H and formation of a B(8)–C(12) bond.

Although there is clear evidence of slight slippage [19] of Rh(2) towards C(12) and C(22), the two C_9 ligands are both essentially η^5-bonded to metal. Their bonding faces are virtually parallel (dihedral angle 2.7°), are separated by 3.56 Å and are disposed relative to each other in a near *cis*-eclipsed conformation, the dihedral angle between planes through C(12)Rh(2)Z(1) and C(22)Rh(2)Z(2) (Z(1) is the mid-point of the C(14)–C(19) bond, Z(2) the mid-point of the C(24)–C(29) bond) being only 17.2° (which may be compared with values of 5.2° and 13.0° in the two crystallographically independent molecules of $(\eta-C_9H_7)_2Fe$ [20]).

The two carbaborane cages lie *cisoid* with respect to each other (this conclusion is valid even though C(2′) is equally disordered between the (2′) and (4′) sites), the term *cisoid* implying a mutually staggered conformation, and Rh(3) is essentially

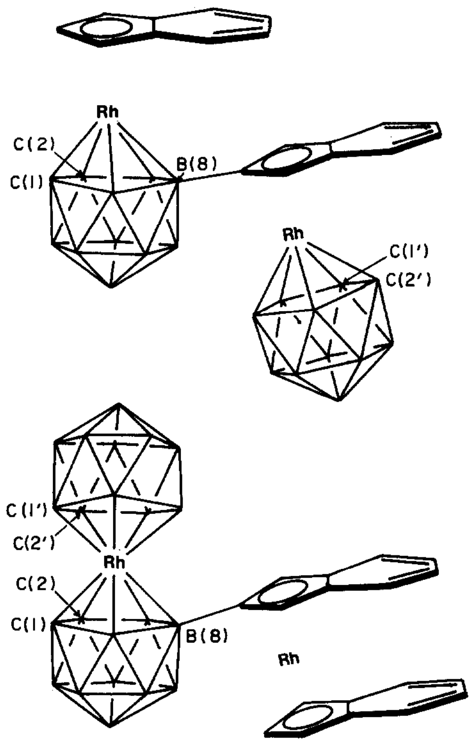

Fig. 1. Possible structures of compound **Ia** based on spectroscopic data (H atoms omitted).

symmetrically bonded to each cage, the unslipped *cisoid* structure being fully expected for a bis(carbaborane) complex of a d^6 metal atom [21]. The metalla-bonded C_2B_3 faces are almost parallel (dihedral angle 6.7°) and are 3.17 Å apart; the staggered conformation of the cages compared to the near eclipsed conformation of the indenyl ligands, given a comparable inter-ligand distance, is attributed to the mutual influence of the inclined substituents, H and $[(C_9H_6)Rh(C_9H_7)]$, of the former.

The second compound isolated from the reaction between $[(C_9H_7)RhCl_2]_x$ and $Tl_2[7,8\text{-}nido\text{-}C_2B_9H_{11}]$ was the apricot-coloured, microcrystalline species **IIa**. ^1H NMR spectroscopy quickly revealed the presence of both (C_9H_7) and (C_9H_6) ligands, as with **Ia**, but only a single broad peak, of integral 2H, was observed in the region associated with cage C*H* nuclei. A notable feature of the ^1H spectrum was a very broad quartet (integral 1H) centred on −1.5 ppm, typical of a BH_{endo} resonance. In the ^{11}B-{^1H} NMR spectrum, six signals were observed (integrals 2:2:1:2:1:1), with chemical shifts between −9 and −40 ppm. On retention of proton coupling, the second lowest frequency signal does not become a doublet, rather it broadens by a factor of *ca.* 2. The ^1H NMR signal at −1.5 ppm is significantly enhanced by irradiation at the ^{11}B frequency of the unique boron atom, and weakly by irradiation at that corresponding to the ^{11}B resonance at δ −9.60 ppm.

Table 2

Coordinates of refined atoms in **Ia**

	x	y	z
Rh(3)	0.5469(4)	0.15023(21)	0.55028(15)
Rh(2)	0.8428(4)	−0.00823(21)	0.63556(16)
C(12)	0.743(6)	0.057(3)	0.5909(18)
C(13)	0.838(6)	0.084(3)	0.6036(19)
C(11)	0.773(5)	0.000(3)	0.5687(17)
C(19)	0.889(5)	−0.015(3)	0.5607(20)
C(18)	0.951(5)	−0.057(3)	0.5419(20)
C(14)	0.925(5)	0.050(3)	0.5859(20)
C(15)	1.048(5)	0.058(3)	0.5864(19)
C(16)	1.109(5)	0.008(3)	0.5669(18)
C(17)	1.067(5)	−0.046(3)	0.5463(20)
C(23)	0.839(5)	0.007(3)	0.7094(17)
C(22)	0.766(5)	−0.047(3)	0.6938(17)
C(21)	0.820(4)	−0.102(3)	0.6709(19)
C(24)	0.948(6)	−0.026(3)	0.6983(19)
C(29)	0.935(5)	−0.087(3)	0.6726(19)
C(25)	1.053(5)	−0.007(3)	0.7026(19)
C(26)	1.129(5)	−0.033(3)	0.6804(19)
C(27)	1.113(5)	−0.095(3)	0.6630(18)
C(28)	1.018(5)	−0.125(3)	0.6561(18)
C(1)	0.448(4)	0.1711(25)	0.6095(18)
C(2)	0.403(4)	0.108(3)	0.5800(19)
B(5)	0.468(5)	0.156(3)	0.6650(23)
B(9)	0.593(5)	0.091(3)	0.6610(23)
B(4)	0.573(5)	0.156(3)	0.6182(23)
B(7)	0.504(5)	0.040(3)	0.5653(23)
B(6)	0.357(5)	0.111(3)	0.6375(25)
B(11)	0.395(5)	0.036(3)	0.6137(25)
B(8)	0.631(6)	0.088(3)	0.5985(25)
B(12)	0.542(5)	0.018(3)	0.6324(24)
B(10)	0.438(6)	0.064(3)	0.6696(24)
C(1′)	0.469(4)	0.2149(24)	0.4969(18)
C/B(2′)	0.534(5)	0.141(3)	0.4706(20)
C/B(4′)	0.564(5)	0.258(3)	0.5296(21)
B(11′)	0.628(5)	0.156(3)	0.4348(23)
B(6′)	0.507(5)	0.215(3)	0.4358(22)
B(5′)	0.521(5)	0.285(3)	0.4625(22)
B(9′)	0.679(5)	0.276(3)	0.4888(24)
B(7′)	0.664(5)	0.133(3)	0.4942(23)
B(8′)	0.699(5)	0.203(3)	0.5295(23)
B(10′)	0.639(5)	0.240(3)	0.4324(23)
B(12′)	0.735(6)	0.200(3)	0.4631(22)
CX(1)	0.628(8)	0.290(5)	0.282(3)
CX(2)	0.476(8)	0.273(5)	0.309(3)
CX(3)	0.577(8)	0.237(6)	0.281(3)
CX(4)	0.522(8)	0.314(5)	0.294(3)
CX(5)	0.670(8)	0.226(5)	0.286(3)
CX(6)	0.583(7)	0.174(5)	0.284(3)
CX(7)	0.384(7)	0.243(5)	0.292(3)
CX(8)	0.463(8)	0.179(4)	0.296(3)

Table 3

Interionic distances (Å) and selected interbond angles (deg) in **Ia**

Rh(3)–C(1)	2.15(5)	C(1)–C(2)	1.61(8)
Rh(3)–C(2)	2.14(5)	C(1)–B(5)	1.65(8)
Rh(3)–B(4)	2.00(7)	C(1)–B(4)	1.59(8)
Rh(3)–B(7)	2.27(7)	C(1)–B(6)	1.82(8)
Rh(3)–B(8)	2.13(7)	C(2)–B(6)	1.76(9)
Rh(3)–C(1′)	2.22(5)	C(2)–B(11)	1.73(9)
Rh(3)–C/B(2′)	2.33(6)	B(5)–B(4)	1.88(9)
Rh(3)–C/B(4′)	2.22(6)	B(5)–B(6)	1.82(9)
Rh(3)–B(7′)	2.20(7)	B(5)–B(10)	1.87(9)
Rh(3)–B(8′)	2.23(6)	B(9)–B(4)	1.80(9)
Rh(2)–C(12)	2.20(6)	B(9)–B(8)	1.88(10)
Rh(2)–C(13)	2.05(6)	B(9)–B(12)	1.77(9)
Rh(2)–C(11)	2.13(6)	B(9)–B(10)	1.99(9)
Rh(2)–C(19)	2.25(6)	B(4)–B(8)	1.62(10)
Rh(2)–C(14)	2.10(6)	B(7)–B(11)	1.95(9)
Rh(2)–C(23)	2.17(5)	B(6)–B(11)	1.69(9)
Rh(2)–C(22)	2.08(6)	B(6)–B(10)	1.65(9)
Rh(2)–C(21)	2.14(5)	B(11)–B(12)	1.93(9)
Rh(2)–C(24)	2.26(6)	B(11)–B(10)	1.79(9)
Rh(2)–C(29)	2.20(6)	B(12)–B(10)	1.90(9)
C(12)–C(13)	1.34(9)	C(1′)–C/B(4′)	1.73(8)
C(12)–C(11)	1.35(8)	C(1′)–B(5′)	1.68(8)
C(12)–B(8)	1.52(9)	C/B(2′)–B(11′)	1.59(9)
C(13)–C(14)	1.37(8)	C/B(2′)–B(6′)	1.81(9)
C(11)–C(19)	1.48(8)	C/B(2′)–B(7′)	1.75(9)
C(19)–C(18)	1.25(8)	C/B(4′)–B(5′)	1.82(9)
C(19)–C(14)	1.54(8)	C/B(4′)–B(9′)	1.88(9)
C(18)–C(17)	1.46(8)	C/B(4′)–B(8′)	1.99(9)
C(14)–C(15)	1.52(8)	B(11′)–B(6′)	1.89(9)
C(15)–C(16)	1.36(8)	B(11′)–B(7′)	1.84(9)
C(16)–C(17)	1.33(8)	B(11′)–B(10′)	1.67(9)
C(23)–C(22)	1.45(8)	B(11′)–B(12′)	1.78(9)
C(23)–C(24)	1.52(8)	B(6′)–B(5′)	1.75(9)
C(22)–C(21)	1.44(8)	B(6′)–B(10′)	1.70(9)
C(21)–C(29)	1.46(8)	B(9′)–B(8′)	1.88(9)
C(24)–C(29)	1.42(8)	B(9′)–B(10′)	1.85(9)
C(24)–C(25)	1.35(8)	B(9′)–B(12′)	1.81(9)
C(29)–C(28)	1.35(8)	B(7′)–B(8′)	1.77(9)
C(25)–C(26)	1.25(8)	B(7′)–B(12′)	1.82(9)
C(26)–C(27)	1.33(8)	B(8′)–B(12′)	1.98(9)
C(27)–C(28)	1.33(8)	B(10′)–B(12′)	1.69(9)
C(1)–Rh(3)–C(2)	43.9(20)	C(1)–C(2)–B(6)	65.3(35)
C(1)–Rh(3)–B(4)	44.9(23)	B(6)–C(2)–B(11)	57.8(35)
C(2)–Rh(3)–B(7)	50.3(22)	C(1)–B(5)–B(4)	53.1(33)
B(4)–Rh(3)–B(8)	46.1(27)	C(1)–B(5)–B(6)	63.1(36)
B(7)–Rh(3)–B(8)	55.7(25)	B(6)–B(5)–B(10)	53.2(35)
C(1′)–Rh(3)–C/B(2′)	47.4(20)	B(4)–B(9)–B(8)	52.4(35)
C(1′)–Rh(3)–C/B(4′)	45.8(20)	B(8)–B(9)–B(12)	66.6(38)
C/B(2′)–Rh(3)–B(7′)	45.3(23)	B(12)–B(9)–B(10)	60.2(35)
C/B(4′)–Rh(3)–B(8′)	53.1(23)	Rh(3)–B(4)–C(1)	72.5(31)
B(7′)–Rh(3)–B(8′)	47.0(24)	Rh(3)–B(4)–B(8)	71.1(35)
C(1)–Rh(3)–C(1′)	101.7(19)	C(1)–B(4)–B(5)	56.1(34)
C(1)–Rh(3)–C/B(4′)	95.0(21)	B(5)–B(4)–B(9)	66.3(37)
C(2)–Rh(3)–C(1′)	98.3(19)	B(9)–B(4)–B(8)	66.3(40)
C(2)–Rh(3)–C/B(2′)	108.3(21)	C(1)–B(6)–C(2)	53.2(31)
B(4)–Rh(3)–C/B(4′)	101.4(24)	C(1)–B(6)–B(5)	54.1(33)

Table 3 (continued)

B(4)–Rh(3)–B(8′)	96.1(25)	C(2)–B(6)–B(11)	60.2(36)
B(7)–Rh(3)–C/B(2′)	95.7(22)	B(5)–B(6)–B(10)	65.2(39)
B(7)–Rh(3)–B(7′)	98.7(24)	B(11)–B(6)–B(10)	65.0(41)
B(8)–Rh(3)–B(7′)	94.6(25)	C(2)–B(11)–B(7)	61.1(34)
B(8)–Rh(3)–B(8′)	92.4(25)	C(2)–B(11)–B(6)	62.0(37)
C(12)–Rh(2)–C(13)	36.6(23)	B(7)–B(11)–B(12)	63.9(34)
C(12)–Rh(2)–C(11)	36.4(22)	B(6)–B(11)–B(10)	56.5(38)
C(13)–Rh(2)–C(14)	38.5(23)	B(12)–B(11)–B(10)	61.2(36)
C(11)–Rh(2)–C(19)	39.3(21)	Rh(3)–B(8)–B(4)	62.8(33)
C(19)–Rh(2)–C(14)	41.3(22)	B(9)–B(8)–B(4)	61.2(39)
C(23)–Rh(2)–C(22)	39.9(21)	B(9)–B(12)–B(10)	65.7(37)
C(23)–Rh(2)–C(24)	40.2(21)	B(11)–B(12)–B(10)	55.9(34)
C(22)–Rh(2)–C(21)	40.0(21)	B(5)–B(10)–B(9)	62.6(35)
C(21)–Rh(2)–C(29)	39.3(21)	B(5)–B(10)–B(6)	61.7(38)
C(24)–Rh(2)–C(29)	37.2(22)	B(9)–B(10)–B(12)	54.0(33)
C(13)–Rh(2)–C(23)	109.0(22)	B(6)–B(10)–B(11)	58.6(38)
C(12)–Rh(2)–C(23)	119.4(22)	B(11)–B(10)–B(12)	62.9(36)
C(12)–Rh(2)–C(22)	115.9(22)	Rh(3)–C(1′)–C/B(4′)	66.9(26)
C(13)–Rh(2)–C(24)	121.1(23)	C/B(4′)–C(1′)–B(5′)	64.6(35)
C(11)–Rh(2)–C(22)	125.7(22)	Rh(3)–C/B(2′)–B(7′)	63.6(28)
C(11)–Rh(2)–C(21)	116.5(21)	B(11′)–C/B(2′)–B(6′)	67.4(39)
C(19)–Rh(2)–C(21)	116.5(21)	B(11′)–C/B(2′)–B(7′)	66.5(39)
C(19)–Rh(2)–C(29)	107.5(21)	Rh(3)–C/B(4′)–C(1′)	67.3(26)
C(14)–Rh(2)–C(24)	111.0(22)	Rh(3)–C/B(4′)–B(8′)	63.6(26)
C(14)–Rh(2)–C(29)	118.0(22)	C(1′)–C/B(4′)–B(5′)	56.4(32)
C(13)–C(12)–C(11)	103.2(54)	B(5′)–C/B(4′)–B(9′)	65.8(35)
C(13)–C(12)–B(8)	126.2(57)	B(9′)–C/B(4′)–B(8′)	58.0(32)
C(11)–C(12)–B(8)	130.6(57)	C/B(2′)–B(11′)–B(6′)	61.9(37)
C(12)–C(13)–C(14)	112.5(55)	C/B(2′)–B(11′)–B(7′)	61.0(38)
C(12)–C(11)–C(19)	120.2(52)	B(6′)–B(11′)–B(10′)	56.7(36)
C(11)–C(19)–C(18)	142.0(58)	B(7′)–B(11′)–B(12′)	60.3(36)
C(11)–C(19)–C(14)	92.5(45)	B(10′)–B(11′)–B(12′)	58.5(38)
C(18)–C(19)–C(14)	125.5(55)	C/B(2′)–B(6′)–B(11′)	50.7(33)
C(19)–C(18)–C(17)	117.6(54)	B(11′)–B(6′)–B(10′)	55.0(35)
C(13)–C(14)–C(19)	111.2(51)	B(5′)–B(6′)–B(10′)	73.2(40)
C(13)–C(14)–C(15)	136.4(55)	C(1′)–B(5′)–C/B(4′)	59.0(33)
C(19)–C(14)–C(15)	112.3(48)	C(1′)–B(5′)–B(6′)	64.7(36)
C(14)–C(15)–C(16)	118.0(52)	C/B(4′)–B(9′)–B(8′)	63.7(34)
C(15)–C(16)–C(17)	123.6(54)	B(8′)–B(9′)–B(12′)	64.8(36)
C(18)–C(17)–C(16)	122.8(52)	B(10′)–B(9′)–B(12′)	54.8(35)
C(22)–C(23)–C(24)	100.1(45)	Rh(3)–B(7′)–C/B(2′)	71.0(30)
C(23)–C(22)–C(21)	114.5(48)	Rh(3)–B(7′)–B(8′)	67.1(30)
C(22)–C(21)–C(29)	105.6(47)	C/B(2′)–B(7′)–B(11′)	52.5(34)
C(23)–C(24)–C(29)	111.5(50)	B(11′)–B(7′)–B(12′)	58.2(35)
C(23)–C(24)–C(25)	135.5(55)	B(8′)–B(7′)–B(12′)	67.0(37)
C(29)–C(24)–C(25)	112.5(54)	Rh(3)–B(8′)–C/B(4′)	63.3(25)
C(21)–C(29)–C(24)	107.7(50)	Rh(3)–B(8′)–B(7′)	65.9(30)
C(21)–C(29)–C(28)	127.0(53)	C/B(4′)–B(8′)–B(9′)	58.2(32)
C(24)–C(29)–C(28)	125.1(55)	B(9′)–B(8′)–B(12′)	56.0(33)
C(24)–C(25)–C(26)	123.9(58)	B(7′)–B(8′)–B(12′)	57.7(34)
C(25)–C(26)–C(27)	117.6(57)	B(11′)–B(10′)–B(6′)	68.4(40)
C(26)–C(27)–C(28)	126.4(55)	B(11′)–B(10′)–B(12′)	63.9(40)
C(29)–C(28)–C(27)	111.1(52)	B(9′)–B(10′)–B(12′)	61.5(37)
Rh(3)–C(1)–C(2)	67.7(27)	B(11′)–B(12′)–B(7′)	61.4(37)
Rh(3)–C(1)–B(4)	62.6(29)	B(11′)–B(12′)–B(10′)	57.5(37)
C(2)–C(1)–B(6)	61.5(34)	B(9′)–B(12′)–B(8′)	59.2(34)
B(5)–C(1)–B(4)	70.7(39)	B(9′)–B(12′)–B(10′)	63.6(38)
B(5)–C(1)–B(6)	62.8(36)	B(7′)–B(12′)–B(8′)	55.3(33)
Rh(3)–C(2)–C(1)	68.4(27)		

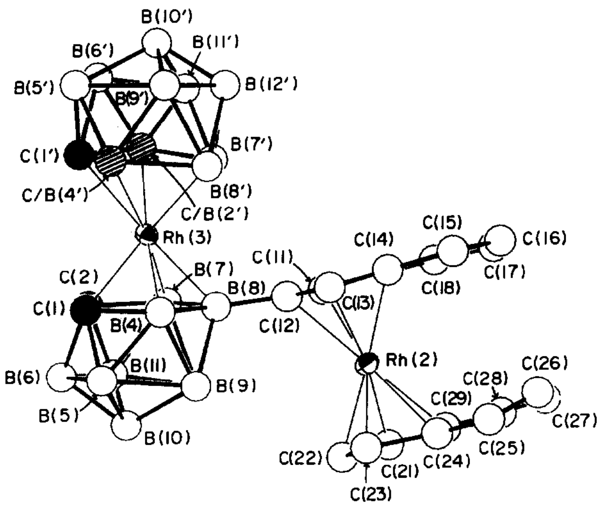

Fig. 2. Crystallographically determined structure of **Ia** with atom numbering. Cage C atoms are shown in black, and disordered C/B atoms are hatched. H atoms have been omitted for clarity. B(12) is totally obscured by B(9) and C(19) is totally obscured by C(14).

Taken together, these spectroscopic data identify compound **IIa** as 10-{$(C_9H_6)Rh(C_9H_7)$}-7,8-*nido*-$C_2H_9H_{11}$, the proposed structure of which is illustrated in Fig. 3. Microanalytical data support this formulation assuming 0.5 mol of CH_2Cl_2 solvate. **IIa** is also zwitterionic, and may be viewed as derived from [7,8-*nido*-$C_2B_9H_{12}]^-$ and $[Rh(C_9H_7)_2]^+$ by loss of 2H and formation of a B(10)–C bond. [7,8-*nido*-$C_2B_9H_{12}]^-$ has been known for many years [22] but has only recently been structurally characterized [23]. The pattern of ^{11}B chemical shifts in **IIa** closely follows that in [7,8-*nido*-$C_2B_9H_{12}]^-$, and the former were assigned by comparison with the latter. All in **IIa** are found to be within 1 ppm of the corresponding resonances in the unsubstituted parent, except for that due to B(10), which experiences a 6 ppm downfield shift on substitution, that due to B(5) and B(6) (adjacent to B(8)), which experiences a complementary upfield shift of 3 ppm and that due to the antipodal atom B(3), which shifts upfield by 1.5 ppm.

The third product of the reaction, **IIIa**, is closely related to that of the novel compound **IIa**, the essential difference being that the carbaborane cage is substituted at B(9). Thus, **IIIa** is 9-{$(C_9H_6)Rh(C_9H_7)$}-7,8-*nido*-$C_2B_9H_{11}$, the proposed structure of which is shown in Fig. 4.

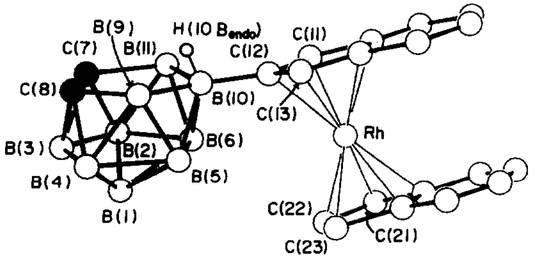

Fig. 3. Proposed structure of **IIa** with all H atoms except H(10B_{endo}) omitted.

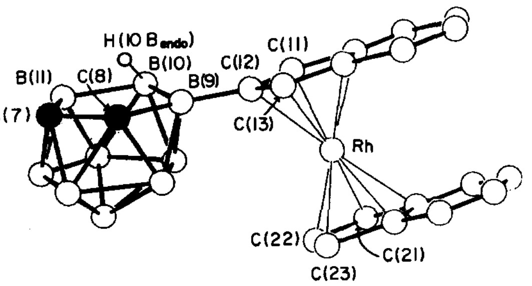

Fig. 4. Proposed structure of **IIIa** with all H atoms except $H(10B_{endo})$ omitted.

The asymmetry in **IIIA** results in two singlets (due to H(11) and H(13)) and two doublets (H(21) and H(23)), each of integral 1, in the high frequency region of the ^1H NMR spectrum, that cannot be mutually distinguished. Moreover, the resonance due to H(22) is seen as a doublet of doublets (almost apparent triplet), and there are two broad singlets, between 2.5 and 2.0 ppm, due to the cage C*H* nuclei, that cannot be specifically assigned. The resonance due to $H(10B_{endo})$ occurs as a broad hump with no discernable structure centred on −2.6 ppm, but this atom may properly be described as *endo* and not bridging since comparison of the ^{11}B-{^1H} and ^{11}B NMR spectra reveals that only one of the ^{11}B resonances that display exopolyhedral doublet coupling (that at −29.45 ppm, assigned to B(10)) is additionally broadened; moreover, only irradiation at the frequency corresponding to the B(10) resonance causes significant enhancement of the −2.6 ppm ^1H signal. The ^{11}B-{^1H} spectrum further reflects the asymmetry of the molecule in showing nine peaks of equal integral, the highest frequency signal being assigned to B(9) because it remains a singlet in the ^{11}B spectrum.

Reaction of $[(C_9H_7)RhCl_2]_x$ with $Tl_2[7\text{-}(CH_2OCH_3)\text{-}7,8\text{-}nido\text{-}C_2B_9H_{10}]$ under conditions similar to those employed for the reaction with $Tl_2[7,8\text{-}nido\text{-}C_2B_9H_{11}]$ (albeit for a somewhat shorter time) affords, after work-up, a single product in low yield. This was isolated as the CH_2Cl_2 solvate (1:1) of $7\text{-}CH_2OCH_3\text{-}10\text{-}\{(C_9H_6)Rh(C_9H_7)\}\text{-}7,8\text{-}nido\text{-}C_2B_9H_{10}$ (**IIb**) and was characterized spectroscopically.

Thus the aromatic region of the ^1H NMR spectrum gave the characteristic signals of the $\{(C_9H_6)Rh(C_9H_7)\}$ moiety, although, in CD_2Cl_2 solution, the multiplet due to H(22) was coincident with both of the signals due to H(11) and H(13), at δ 5.92 ppm. In $(CD_3)_2CO$, however, the doublet of doublets due to H(22) was relatively shifted to low frequency, and, moreover, its assignment was confirmed since it collapsed to a singlet upon irradiation at the frequency corresponding to the resonance due to H(21,22). Also of note in the ^1H spectrum was the AB pattern due to the CH_2 protons of the ether substituent [10,24] and a very broad quartet centred on −1.4 ppm characteristic of a BH_{endo} nucleus.

The ^{11}B-{^1H} and ^{11}B NMR spectra were fully consistent with the proposed formulation, there being nine signals in the former between −4 and −36 ppm, with that at second lowest frequency broadening in the latter. Thus the boron atom that carries a terminal substituent (the $(C_9H_6)Rh(C_9H_7)$ unit) is also associated with a non-exopolyhedral H atom. The similarity of the chemical shift of this resonance to that of the similar signals in $[7,8\text{-}nido\text{-}C_2B_9H_{12}]^-$ and **IIa** identifies the stereochemistry of the present compound.

Two products were isolated from the prolonged reaction between $[(C_9H_7)RhCl_2]_x$ and $Tl_2[7\text{-}Ph\text{-}7,8\text{-}\textit{nido}\text{-}C_2B_9H_{10}]$. The faster moving olive component was identified as $1\text{-}Ph\text{-}3\text{-}(C_9H_7)\text{-}3,1,2\text{-}\textit{closo}\text{-}RhC_2B_9H_{10}$ (**IVd**) by single crystal X-ray diffraction, being isomorphous with the previously characterized cobalt analogue [2]. The product in the slower moving band was recovered by a recrystallization from CH_2Cl_2 hexane (1 : 4) as orange microcrystals. Its ^1H NMR spectrum reveals that the $\{(C_9H_6)Rh(C_9H_7)\}$ moiety that is clearly present is bound to an asymmetric carbaborane cage, both pairs H(11) and H(13), and H(21) and H(23) being rendered magnetically inequivalent. Note that since only one of the cage carbon atoms carries a phenyl substituent, this spectrum alone does not identify the boron atom that is substituted. However, of the eight resonances in the $^{11}B\text{-}\{^1H\}$ NMR spectrum, all those at low frequency show clear exopolyhedral doublet coupling in the ^{11}B spectrum (the second lowest frequency signal displaying additional broadening, and thus assignable to B(10)). Indeed, it is one component of the highest frequency coincidence that remains a singlet in the coupled spectrum. Thus the combined spectroscopic data identify the compound as $7\text{-}Ph\text{-}9/11\text{-}\{(C_9H_6)Rh(C_9H_7)\}\text{-}7,8\text{-}\textit{nido}\text{-}C_2B_9H_{10}$ (**IIId**) in which we are unable to distinguish between substitution by the $\{(C_9H_6)Rh(C_9H_7)\}$ unit at either B(9) or B(11).

In the final reaction undertaken, a mixture of $[(C_9H_7)RhCl_2]_x$ and $Tl_2[7,8\text{-}(CH_2OCH_3)_2\text{-}7,8\text{-}\textit{nido}\text{-}C_2B_9H_9]$ in CH_2Cl_2 was stirred overnight. Work-up afforded a very low yield of a single mobile species, subsequently isolated as dark yellow microcrystals.

$^{11}B\text{-}\{^1H\}/^{11}B$ NMR spectroscopy revealed six signals of relative integral 1 : 1 : 2 : 2 : 2 : 1, in the chemical shift range δ +10 to −20 ppm, all of which showed clear doublet coupling, thus indicating a $3,1,2\text{-}\textit{closo}\text{-}MC_2B_9$ polyhedron. Moreover, the ^1H NMR spectrum suggested a single (C_9H_7) ligand, with signals in the ratio 4 : 2 : 1 corresponding to H(35–38), H(31,33) and H(32) respectively. Thus the

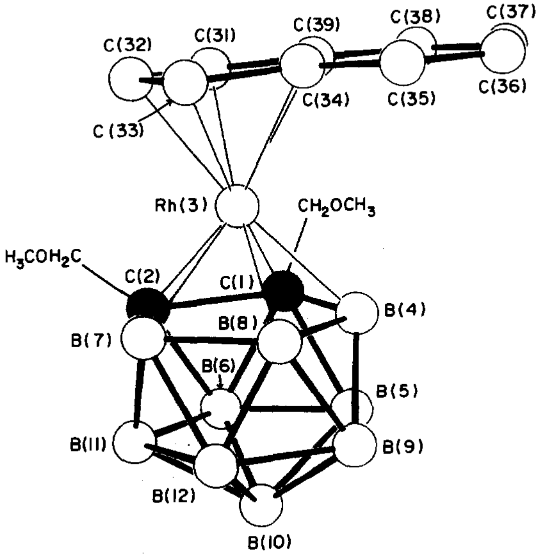

Fig. 5. Proposed structure of IVc with H atoms omitted.

Compound type		Examples
I	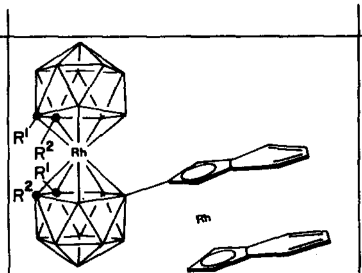	Ia
II	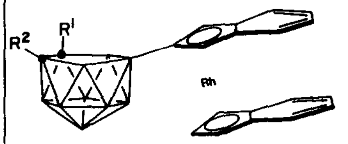	IIa IIb
III	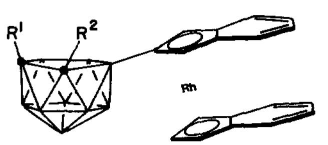	IIIa IIId*
IV	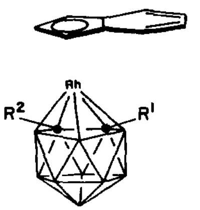	IVc IVd

Scheme 1. (a) $R^1 = R^2 = H$; (b) $R^1 = CH_2OCH_3$, $R^2 = H$; (c) $R^1 = R^2 = CH_2OCH_3$; (d) $R^1 = Ph$, $R^2 = H$. * In **IIId**, the relative positions of R^1 and R^2 are not established.

compound is identified as 1,2-$(CH_2OCH_3)_2$-3-(C_9H_7)-3,1,2-*closo*-$RhC_2B_9H_9$ (**IVc**), the proposed structure of which is shown in Fig. 5. Indeed, both the ^{11}B and ^1H NMR spectra of **IVc** are closely similar to those of the cobalt analogue 1,2-$(CH_2OCH_3)_2$-3-(C_9H_7)-3,1,2-*closo*-$CoC_2B_9H_9$ which has been studied crystallographically [2].

Conclusions

A variety of novel rhodium carbaborane compounds **I–IV** (Scheme 1) have been isolated from the reactions between $[(C_9H_7)RhCl_2]_x$ and thallium salts of the *nido* carbaborane anions $[7\text{-}R'\text{-}8\text{-}R''\text{-}7,8\text{-}nido\text{-}C_2B_9H_9]^{2-}$. In **I**, a {*closo*-$Rh(C_2B_9)_2$} and a {$(C_9H_6)Rh(C_9H_7)$} fragment are fused *via* a B(8)–C bond, whereas in **II** and **III**, the bis(indenyl)Rh unit is attached to *nido*-C_2B_9 cages by B–C bonds either at B(10) or at B(9/11) (note the different numbering conventions [25] for *closo* and *nido* icosahedral heteroboranes). Compounds **IV**, on the other hand, are conventional indenyl carbametallaboranes [1,2], structural analogues of previously characterized cobalt species.

It is possible that **I** may be obtained only with the underivatized carbaborane cage for steric reasons, and it is of interest that compounds **IV** were isolated after relatively long reaction times (*ca.* 15 h *cf.* 1–2.5 h for **I–III**) possibly suggesting a degree of kinetic control in these reactions. One major problem is that all these products are formed in low yields; in part this may be a consequence of both the insolubility of Tl_2[carbaborane] species and the limited solubility of $[(C_9H_7)RhCl_2]_x$ in CH_2Cl_2, and thus future studies in this area are likely to employ soluble salts of $[7,8\text{-}nido\text{-}C_2B_9H_{11}]^{2-}$ and its derivatives, either pre-prepared or generated *in situ*.

To a limited extent, the identification of these unusual rhodium carbaborane compounds allows some speculation as to the nature of the precursor $[(C_9H_7)RhCl_2]_x$. It clearly possesses a more complicated structure than either $[CpRhCl_2]_x$ or $[Cp^*RhCl_2]_2$; indeed, its partial solubility in organic solvents suggests that it may not even be a homogeneous material, even though the synthesis and microanalytical data are fully reproducible. Interestingly the CD_2Cl_2 soluble portion of $[(C_9H_7)RhCl_2]_x$ exhibits signals in the ^1H NMR spectrum which may be attributed to (C_9H_7) and (C_9H_6) groups, by analogy with those observed in **I–IV**, but it is not known whether these units are bound to the same or different rhodium atoms, nor what is additionally σ-bonded to C(12) (to use the numbering system adopted for **I–III**) of the (C_9H_6) ligand. Moreover, the ^1H spectrum above contains a number of other (unassigned) signals and this in any case only represents the methylene chloride soluble portion of $[(C_9H_7)RhCl_2]_x$.

We are continuing our studies into this interesting and potentially useful organometallic reagent.

Acknowledgments

We thank the DENI for support (ZGL), Dr. D. Reed for NMR spectra and helpful discussions, the Callery Chemical Company for a generous gift of $B_{10}H_{14}$, and Johnson Matthey plc for a loan of rhodium trichloride.

References

1 D.E. Smith and A.J. Welch, Organometallics, 5 (1986) 760.
2 Z.G. Lewis, D. Reed and A.J. Welch, J. Chem. Soc., Dalton Trans., (1992) 731.
3 C.J. Jones and M.F. Hawthorne, Inorg. Chem., 12 (1973) 608.
4 R.J. Angelici and E.D. Fisher, J. Am. Chem. Soc., 85 (1963) 3733.
5 J.W. Kang, K. Mosely and P.M. Maitlis, J. Am. Chem. Soc., 91 (1969) 5970.
6 T.P. Hanusa and L.J. Todd, Polyhedron, 4 (1985) 2063.
7 X.L.R. Fontaine, H. Fowkes, N.N. Greenwood, J.D. Kennedy and M. Thornton-Pett, J. Chem. Soc., Dalton Trans., (1986) 547.
8 X.L.R. Fontaine, N.N. Greenwood, J.D. Kennedy, K. Nestor, M. Thornton-Pett, S. Hermanek, T. Jelinek and B. Stibr, J. Chem. Soc., Dalton Trans., (1990) 681.
9 M.P. Garcia, M. Green, F.G.A. Stone, R.G. Somerville, A.J. Welch, C.E. Briant, D.N. Cox and D.M.P. Mingos, J. Chem. Soc., Dalton Trans., (1985) 2343.
10 K.F. Shaw and A.J. Welch, Polyhedron, 11 (1992) 157.

11 B.D. Reid and A.J. Welch, unpublished results.

12 G.M. Sheldrick, University of Gottingen, 1986.

13 G.M. Sheldrick, University of Cambridge, 1976.

14 International Tables for X-Ray Crystallography, Kynoch Press, Birmingham, Vol. 4, 1974, p. 99.

15 R.O. Gould and D.E. Smith, University of Edinburgh, 1986.

16 N.G. Walker and D. Stuart, Acta Crystallogr., Sect. A, 39 (1983) 158.

17 R.O. Gould and P. Taylor, University of Edinburgh, 1986.

18 P. Mallinson and K.W. Muir, J. Appl. Crystallogr., 18 (1985) 51.

19 D.M.P. Mingos, M.I. Forsyth and A.J. Welch, J. Chem. Soc., Dalton Trans., (1978) 1316.

20 S.A. Westcott, A.A. Kakkar, G. Stringer, N.J. Taylor and T.B. Marder, J. Organomet. Chem., 394 (1990) 777.

21 D.M.P. Mingos and M.I. Forsyth, J. Organomet. Chem., 146 (1978) C37.

22 M.F. Hawthorne, D.C. Young, P.M. Garrett, D.A. Owen, S.G. Schwerin, F.N. Tebbe and P.A. Wegner, J. Am. Chem. Soc., 90 (1968) 862.

23 J. Buchanan, E.J.M. Hamilton, D. Reed and A.J. Welch, J. Chem. Soc., Dalton Trans., (1990) 677.

24 K.F. Shaw and A.J. Welch, Polyhedron, in preparation.

25 J.B. Casey, W.J. Evans and W.H. Powell, Inorg. Chem., 22 (1983) 2228.